ARTICLE IN PRESS

Marine Chemistry xxx (xxxx) xxxx

FISFVIFR

Contents lists available at ScienceDirect

Marine Chemistry

journal homepage: www.elsevier.com/locate/marchem



Investigating the cycling of chromium in the oxygen deficient waters of the Eastern Tropical North Pacific Ocean and the Santa Barbara Basin using stable isotopes

Simone B. Moos^{a,b}, Edward A. Boyle^{a,*}, Mark A. Altabet^c, Annie Bourbonnais^d

- ^a Department of Earth, Atmospheric, and Planetary Sciences, Massachusetts Institute of Technology, Cambridge, MA 02139, USA
- ^b Joint Program in Oceanography, Massachusetts Institute of Technology & Woods Hole Oceanographic Institution, USA
- c School for Marine Science and Technology, Department of Estuarine and Ocean Sciences, University of Massachusetts Dartmouth, New Bedford, MA 02747, USA
- ^d School of the Earth, Ocean and Environment, University of South Carolina, Columbia, SC 29208, USA

ARTICLE INFO

Keywords: Chromium isotopes Oxygen depletion Eastern Tropical North Pacific Santa Barbara Basin

ABSTRACT

Cr isotope geochemistry is being explored in the context of a variety of geological problems as well as the environmental remediation of pollutant Cr(VI). There is a strong Cr isotope fractionation during reduction of oxidized Cr(VI) to reduced Cr(III). We present chromium concentration and Cr isotope data for samples from highly reducing environments ([O₂] < 2 µmol/kg) in the Eastern Tropical North Pacific (ETNP) Oxygen Deficient Zone (ODZ) off of Mexico and the deep Santa Barbara Basin off of California. Total dissolvable Cr in the upper ETNP ODZ is slightly depleted (by up to 0.8 nmol/kg) and δ^{53} Cr is up to 0.1–0.2% heavier compared to oxic waters of the same density seen at the SAFe station (30°N, 140°W), presumably both a result of reduction of Cr(VI) and removal of light Cr(III) by sinking particles. The Cr depletion and Cr isotope fractionation peak at the same depth as the highest $\delta^{15}N$ of NO_3^- and decrease within the equally oxygen-deficient waters below, implying that microbial reduction dependent on the sinking organic matter flux may be the mechanism of Cr reduction. These data are consistent with a fractionation mechanism with a net isotope fractionation factor of $\epsilon \approx -0.44\%$. In the deepest anoxic waters of the Santa Barbara Basin in July 2014, dissolved (<0.2 μ m) Cr is depleted by up to 1.8 nmol/kg and δ^{53} Cr is up to 0.5‰ heavier compared to SAFe station waters of the same density. This is consistent with a net isotope fractionation factor of $\varepsilon \approx -0.65\%$. At the Santa Barbara Basin site, it is possible that abiotic Fe(II) reduction (from Fe(II) diffusing out of reducing continental shelf sediments) also contributes to Cr reduction in addition to the microbial reduction mechanism.

1. Introduction

Chromium (Cr) reduction in aqueous systems can generate significant Cr isotope fractionation as the resulting Cr(III) fraction is both isotopically light and more particle-reactive compared to the initial Cr (VI) pool. Isotope effects of different Cr(VI) reduction mechanisms have been characterized in laboratory experiments (e.g. Basu and Johnson, 2012; Døssing et al., 2011; Ellis et al., 2002; Kitchen et al., 2012; Sikora et al., 2008), and Cr(VI) reduction in groundwater has been monitored extensively via stable Cr isotope analyses (e.g. Berna et al., 2010; Ellis et al., 2002; Izbicki et al., 2012). However, oxygen deficient waters of the ocean, which appear to be active sites of Cr reduction (Murray et al., 1983; Rue et al., 1997), have not been studied using a stable Cr isotope approach until recently.

In seawater, Cr exists both in the trivalent form (as a particle-reactive solvated cation and as potential organic complexes; Byrne, 2002) and in the hexavalent form (as the soluble oxyanion chromate, CrO_4^{2-}). While total Cr concentrations range between 1.2 nmol/kg – 6.5 nmol/kg in seawater (e.g. Bonnand et al., 2011; Goring-Harford et al., 2018; Moos and Boyle, 2019; Rickli et al., 2019; Scheiderich et al., 2015), the distribution of the individual redox species is largely a function of oxygen levels, the presence of reductants and oxidants, as well as the kinetics of Cr redox transitions. In accordance with thermodynamic calculations, field studies have found Cr(VI) to be the dominant redox species under oxygenated conditions, while Cr(III) can reach levels above a few tenths of nmol/kg in anoxic environments. Once Cr(III) has been formed, it can persist in the water column on a time scale of months to years due to the kinetics of Cr redox transitions.

E-mail address: eaboyle@mit.edu (E.A. Boyle).

https://doi.org/10.1016/j.marchem.2020.103756

0304-4203/ © 2020 Published by Elsevier B.V.

^{*}Corresponding author at: Department of Earth, Atmospheric, and Planetary Sciences E25-619, Massachusetts Institute of Technology, Cambridge, MA 02139, USA

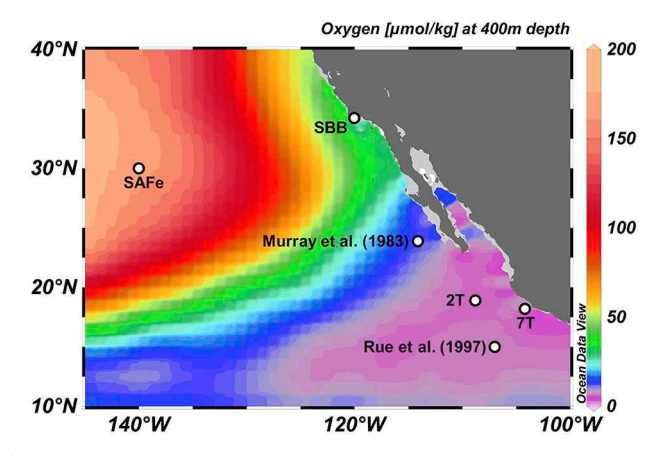


Fig. 1. Sampling locations of stations 2T, 7T, SAFe and SBB (= Santa Barbara Basin) superimposed onto the distribution of oxygen concentrations (μ mol/kg) at 400 m depth. Annual oxygen data in ml/L (1°grid) from the World Ocean Atlas 2009 (WOA09) served as a basis for this plot (Garcia et al., 2010). Original oxygen data was converted to μ mol/kg using an embedded function of Ocean Data View (Schlitzer, 2013), that was also used to make this map. Note that the lowest oxygen concentration at the SAFe station is not found at 400 m but at 864 m (13.2 μ mol/kg). The Santa Barbara Basin exhibits [O₂] < 2.0 μ mol/kg from 532 m to the bottom depth (579 m).

Direct oxidation of Cr(III) by dissolved oxygen (Schroeder and Lee, 1975) and $\rm H_2O_2$ (Pettine and Millero, 1990) is slow. More rapid oxidation has been observed in the presence of $\rm MnO_2$ (Schroeder and Lee, 1975; Van der Weijden and Reith, 1982). In contrast, hexavalent Cr is readily reduced in the presence of electron donors such as organic matter (Rai et al., 1989; Schroeder and Lee, 1975), Fe(II) (Eary and Rai, 1987; Kieber and Helz, 1992; Pettine et al., 1998; Schroeder and Lee, 1975), and reduced sulfur (Pettine et al., 1994). Additionally, photochemical (Kieber and Helz, 1992) and microbially-mediated (Lovley, 1993) reduction of Cr(VI) have been reported. Cr(III) is particle-reactive and can be removed from the water column by sinking particles; Cr(VI) is not particle-reactive.

Oxygen Deficient Zones (ODZs; defined here as oxygen levels below 2 μM) appear to be active reduction sites of Cr(VI) to Cr(III) based on Cr concentration studies conducted in the Eastern Tropical North Pacific (ETNP) Ocean (Fig. 1; Murray et al., 1983; Rue et al., 1997) and in the Saanich Inlet (Emerson et al., 1979). Existing ETNP data indicate that Cr(III) levels peak at 0.9 nmol/kg - 1.0 nmol/kg in the upper ODZ compared to the equally oxygen-deficient deeper ODZ. As the location of the Cr(III) peak is near the 15 N enrichment feature of NO_3^- within ODZs, Cr cycling in ODZs (like N cycling) may be linked to microbial activity dependent on the organic particle flux from above (Voss et al., 2001; Cline & Kaplan, 1975; Altabet et al., 1995; Ward et al., 2009). Rue et al. (1997) noted that their observed Cr(III) peak only accounted for ~50% of the chromate deficit. They attributed the remaining chromate deficit to scavenging and subsequent export of particle-reactive Cr(III). This hypothesis would appear to be supported by the data of Murray et al. (1983) showing up to 1 nmol/kg of particulate Cr at a nearby location within the Mexican ODZ.

This study presents total Cr isotope and concentration measurements associated with two stations within the ETNP ODZ and at a station in the Santa Barbara Basin, which featured an anoxic bottom layer at the time of sampling. We evaluate potential Cr reduction at these 3 stations by comparing them to the Cr profile of the nearby SAFe station (Moos and Boyle, 2019), which features an oxygen-bearing water column ([O2] $\,>\,$ 13.2 $\,\mu$ mol/kg). Since Cr(VI) reduction typically produces isotopically light Cr(III) (e.g. Ellis et al., 2002), a buildup of Cr(III) in the upper ODZ should be isotopically light relative to the initial Cr(VI) pool. If (as implied by Murray et al. (1983) and Rue et al. (1997)) a fraction of the reduced Cr exits the ODZ due to scavenging onto particles, the residual Cr in the upper ODZ should be rendered isotopically heavy. For reference

purposes, the first Cr isotope studies of oxic seawater have reported δ^{53} Cr signatures ranging from 0.41% to 1.55% (Bonnand et al., 2013; Goring-Harford et al., 2018; Moos and Boyle, 2019; Scheiderich et al., 2015). All the oxic Cr isotope data published to date fall on a linear negative δ^{53} Cr – log[Cr] relationship, which Scheiderich et al. (2015) attribute to a closed-system Rayleigh fractionation process with an inferred fractionation factor of -0.8%. Whether or not the anoxic seawater Cr isotope data of our study continues to fall on this δ^{53} Cr – log[Cr] relationship will help us understand, if the process that shapes Cr cycling in anoxic environments has a distinct isotope fractionation from the process that shapes Cr in the previously investigated oxic environments. Furthermore, we intend to evaluate if Cr cycling in anoxic seawater is driven by sinking-flux dependent microbial activity. To this end, we will compare δ^{53} Cr and δ^{15} N of NO₃ $^-$ measurements that were obtained from concurrent sampling of our two ETNP ODZ stations.

2. Methods

2.1. Sample collection

Total dissolvable Cr (TDCr) and Cr isotope sampling to 800 m was conducted at two stations within the Eastern Tropical North Pacific off of Mexico (Fig. 1, stn. 2T: 18.9°N 108.8°W, est. bottom depth 3085 m; stn. 7T: 18.2°N 104.2°W, est. bottom depth 3130 m) during an expedition aboard the R/V *New Horizon* (NH1410, May 2014). After seawater samples were collected with standard Niskin bottles, they were stored unfiltered and then acidified after transport to MIT. Later work on 0.2 µm filtered samples acidified at sea from a nearby station (RR1804-5 P2, 16.9°N 109°W), indicates that particulate Cr at these sites is very low and that later acidification does not affect the total dissolved Cr (see Fig. 5).

An additional full water column profile was collected within the Santa Barbara Basin (Figs. 1 and 2, 34.23°N 120.03°W) on July 24, 2014 during expedition MV1405 on board the R/V Melville. Upon retrieval via teflon coated GO-FLO bottles, the Santa Barbara Basin samples were filtered immediately (0.2 μm AcroPak Supor capsules) and acidified upon arrival at MIT.

2.2. Cr concentration and isotope analyses

Total Cr concentrations and isotope signatures of seawater samples were determined using a technique that has been detailed extensively by Moos and Boyle (2019); therefore, only a brief summary is given here.

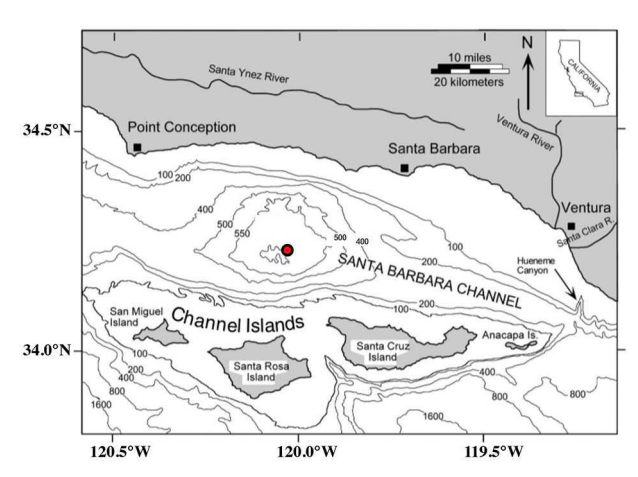


Fig. 2. Bathymetry of the Santa Barbara Basin. The red dot marks our sampling location. (For interpretation of the references to colour in this figure legend, the reader is referred to the web version of this article.)

The acidification of seawater samples to pH 2 prompts the conversion of Cr(VI) to Cr(III) over the course of several months (Semeniuk et al., 2016). In this particular case, all seawater samples were stored at pH~2 for > 2 years. Once the entirety of Cr in the sample is present as Cr(III), a ⁵⁰Cr⁻⁵⁴Cr double spike (also present in the trivalent form) is equilibrated with the sample for 3 days. This double spike addition enables accurate correction of procedural and instrumental mass-dependent Cr mass fractionations (Rudge et al., 2009). Preconcentration of Cr is accomplished by Mg(OH)₂ coprecipitation which is selective for Cr(III) over Cr (VI) (Semeniuk et al., 2016). The resulting Mg(OH)₂ pellet is neutralized with HCl and ultimately brought up in 0.02 M HCl. In preparation for the first ion-exchange column step. Cr is oxidized to Cr(VI) using ammonium persulfate (Götz and Heumann, 1988). This step demands careful pH. temperature and time control due to pitfalls such as the unwanted generation of H₂O₂ (Palme, 1920) and subsequent back-reduction of Cr(VI). Purification from the Mg/seawater matrix is achieved with a 3-anion exchange column scheme (AG1-X8). The first column separates oxyanion CrO₄²⁻ from the matrix cations (mainly Mg⁺⁺) and from isobaric interferences (i.e. V, Ti, Fe) (Ball and Bassett, 2000). Sulfur species, which form anionic polyatomics that interfere with accurate Cr analysis, are removed in a second column run for which Cr passes through the column in the trivalent state. Traces of Fe are eliminated in a third column step with Fe being present as FeCl₄ (Yamakawa et al., 2009) and Cr being present as cationic Cr(III). Abundances of masses 49 (Ti), 50 (Cr,Ti,V), 51 (V), 52 (Cr), 53 (Cr), 54 (Cr, Fe) and 56 (Fe) in purified samples are detected by Faraday cups in low resolution mode on the IsoProbe, a multicollector inductively coupled plasma mass spectrometer (MC-ICP-MS) featuring a hexapole collision cell capable of eliminating many polyatomic interferences using Ar and H2 collision gases. The machine is tuned to maximize the ratio of the Cr signal relative to the polyatomic sulfur signal at mass 49, at the cost of a ~30% loss of Cr signal. Once the true 53Cr/52Cr ratio of a sample is determined, it is compared to the ⁵³Cr/⁵²Cr ratio of bracketing standard reference material 979 (SRM 979) and relative deviations are reported as δ^{53} Cr values in per mil (Eq. (1)). We achieved a δ^{53} Cr 2 σ precision of $\pm 0.06\%$ as indicated by replicate analysis of 3 seawater samples. Running 10 samples of SRM979 through the complete column procedure gave an average of +0.02% with a 2σ standard deviation of 0.06‰, so the accuracy is comparable to the pre-

$$\delta^{53}Cr\left(\%\right) = \left(\frac{\left(\frac{53}{52}Cr\right)_{Sample}}{\left(\frac{53}{52}Cr\right)_{SRM979}} - 1\right) \times 1000$$
(1)

When quantifying the magnitude of an isotope effect, we refer to fractionation factors α , which compares the $^{53}\text{Cr}/^{52}\text{Cr}$ ratio of the product to that of the reactant (Eq. (2)), and ϵ , which compares the $\delta^{53}\text{Cr}$ value of the product to that of the reactant (Eq. (3)). The fractionation factors are approximately linked by Eq. (4).

$$\alpha = \frac{\binom{5^3Cr}{5^2Cr}_{Product}}{\binom{5^3Cr}{5^2Cr}_{Reactant}}$$
(2)

$$\varepsilon(\%) = \delta^{53} C r_{Product} - \delta^{53} C r_{Reactant}$$
(3)

$$\varepsilon(\%) \approx 1000 \times \ln(\alpha) \approx 1000 \times (\alpha - 1)$$
 (4)

2.3. Dissolved nitrate $\delta^{15}N$ analysis

The nitrogen stable isotopic composition $(\delta^{15}N)$ of NO_3^- was analyzed at the University of Massachusetts Dartmouth following the chemical method described in McIlvin and Altabet (2005). 10% of the

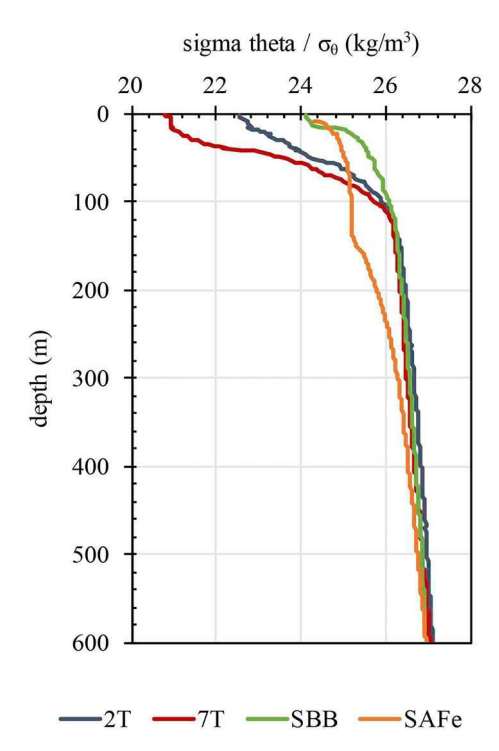
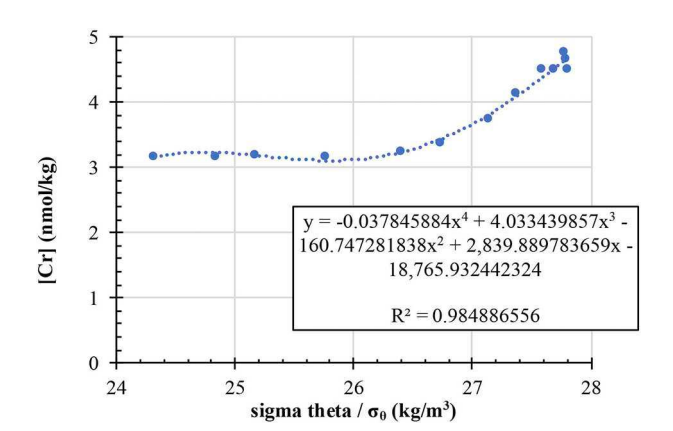


Fig. 3. Upwelling of waters is observed towards the coast of Mexico and California (evidenced by the higher density of waters upwelled from depth).



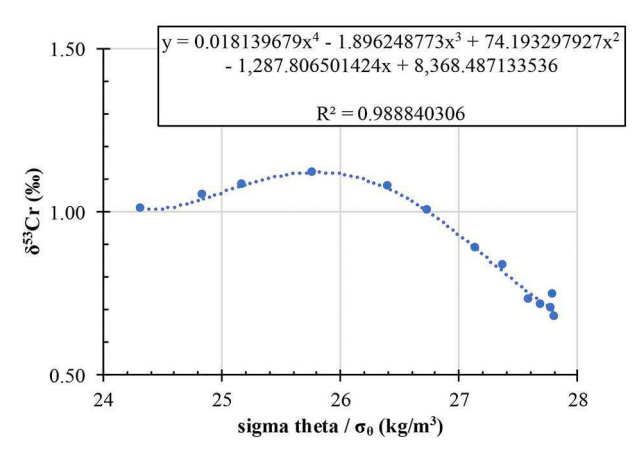


Fig. 4. The [Cr]- σ_{θ} relationship at SAFe is approximated by a 4th-order polynomial (upper panel). Likewise, the δ^{53} Cr - σ_{θ} relationship at SAFe is approximated by a 4th-order polynomial (lower panel).

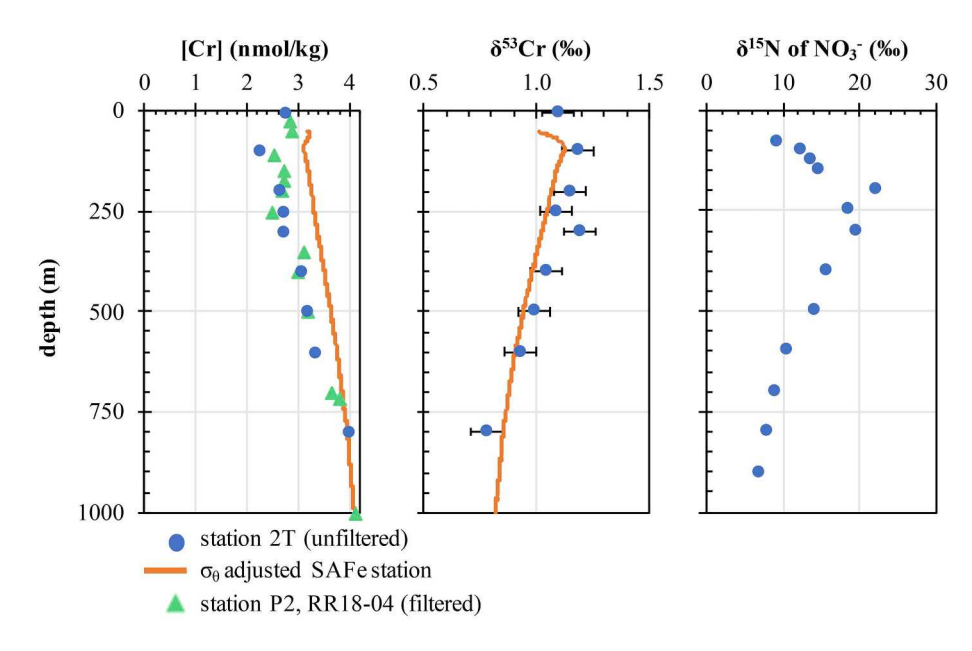
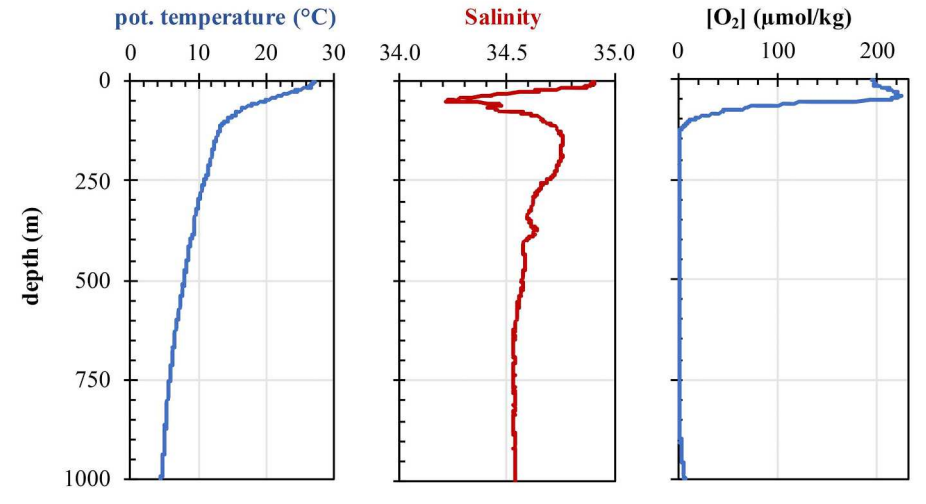


Fig. 5. Full water column profiles for a suite of parameters at station 2T which is located within the ODZ of the Eastern Tropical Pacific. Total dissolvable Cr concentrations and isotope ratios measured at 2T (blue dots) are shown alongside the σ_{θ} adjusted SAFe profiles (orange lines). Error bars of Cr isotope ratios are 2SD. Cr concentration data from 0.2 μm filtered samples from nearby station RR1804–5 P2 (green triangles) are shown for comparison, and indicate that there is at most a few tenths of a $\mu mol/kg$ of particulate Cr at NH1410 station 2T. (For interpretation of the references to colour in this figure legend, the reader is referred to the web version of this article.)



total number of samples were analyzed as duplicates. Cadmium was first used for the reduction of NO_3^- to NO_2^- . NO_2^- was then converted to nitrous oxide (N_2O) using sodium azide in acetic acid. N_2O gas was automatically extracted, purified, and analyzed online using a purgetrap preparation system coupled to an IsoPrime continuous-flow, isotope ratio mass spectrometer (CF-IRMS). The target sample and standard size was 15 nmol N_2O . N and O isotope ratios are reported in per mil (‰), relative to N_2 in air for $\delta^{15}N$ (Eq. (5)):

$$\delta^{15}N = (R_{\text{sample}}/R_{\text{standard}} - 1) * 1000$$
 (5)

, where $R = {}^{15}\text{N}/{}^{14}\text{N}$ and the standard is AIR.

Isotope values were calibrated using the following international references: IAEA N3 ($\delta^{15}{\rm N}=4.7\%$ and $\delta^{18}{\rm O}=25.6\%$), USGS 34 ($\delta^{15}{\rm N}=-1.8\%$ and $\delta^{18}{\rm O}=-27.9\%$), USGS 35 ($\delta^{15}{\rm N}=2.7\%$ and $\delta^{18}{\rm O}=57.5\%$), and an in-house standard (LAB_{mix}, $\delta^{15}{\rm N}=38.9\%$) for NO₃ $^-$ isotopic analysis. Reproducibility was generally better than 0.2%.

3. Results and discussion

3.1. Circulation of the ETNP ODZ and setting up an oxic counterpart

Circulation in the ETNP ODZ is diminished relative to other parts of the ocean because it is in the "shadow zone" of the main potential-vorticity conserving thermocline ventilation mechanism (Luyten et al., 1983). Instead, eddies and jets from outside the ODZ probably irregularly ventilate this region (as seen in the North Atlantic shadow zone, Brandt et al., 2015). Low thermocline oxygen in this region is a result of the limited ventilation aided by the organic matter flux from eastern boundary upwelling. Although WOCE sections only skirted this region, extrapolated ETNP thermocline CFC ventilation ages are \sim 10 years at $\sigma_{\Phi}=25.9$ (\sim 80 m) to \sim 35 years at $\sigma_{\Phi}=27.2$ (\sim 700 m) (Fine et al., 2001).

In order to evaluate the extent of Cr reduction at our 3 partially anoxic stations, we compare their Cr profiles to that of the oxygenbearing SAFe station in the North Pacific (Moos and Boyle, 2019). As we discuss later, a station further away from the ETNP might make for a better comparison, but SAFe is the only regional site with [Cr] and Cr isotope data. Such a direct comparison necessitates that we correct for ETNP upwelling of water towards the coast (Fig. 3) by adjusting SAFe station's Cr data using potential density (σ_{θ}). The [Cr]- σ_{θ} relationship at SAFe can be approximated by a 4th-order polynomial (upper panel of Fig. 4). This relationship is applied to σ_{θ} of the 3 partly anoxic stations and results in the creation of an upwardly shifted and compressed SAFe Cr concentration profile. Likewise, the δ^{53} Cr - σ_{θ} relationship at SAFe can be approximated by a 4th-order polynomial (lower panel of Fig. 4), which is applied to σ_{θ} of the partially oxygen deficient stations to give a σ_{θ} -adjusted SAFe Cr isotope ratio profile. Figs. 5, 6 and 7 show the total Cr concentrations and isotope ratios measured at 2T, 7T and at the Santa Barbara Basin site (blue dots) alongside the σ_{θ} -adjusted SAFe profiles (orange lines).

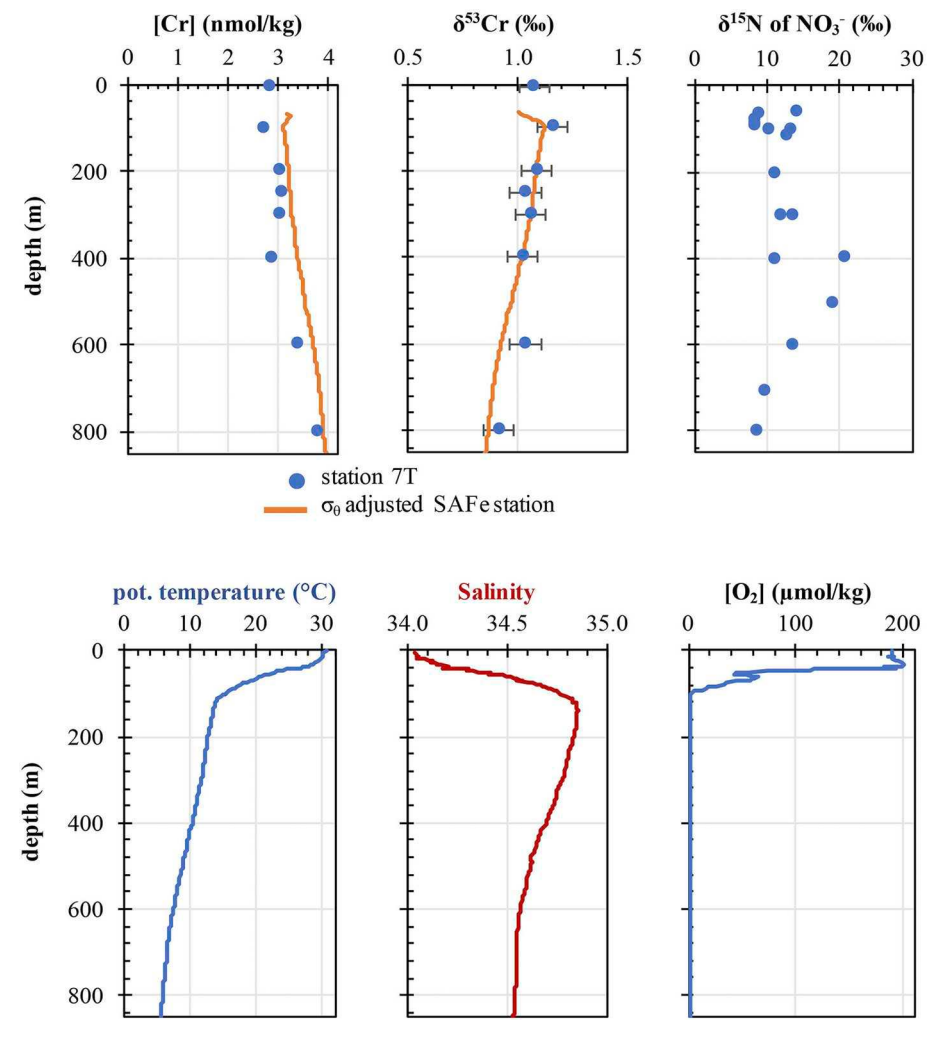


Fig. 6. Full water column profiles for a suite of parameters at station 7T which is located within the ODZ of the Eastern Tropical Pacific. Total Cr concentration and isotope ratios measured at 7T (blue dots) are shown alongside the σ_{θ} adjusted SAFe profiles (orange lines). Error bars of Cr isotope ratios are 2SD. (For interpretation of the references to colour in this figure legend, the reader is referred to the web version of this article.)

3.2. Profiles of Cr and other oceanographic properties

3.2.1. ETNP Ocean

At station 2T, oxygen concentrations drop below 1.6 µmol/kg between 130 m and 820 m depth (Tables 1 and 2, Fig. 5). Measured total dissolvable Cr (= particulate + dissolved) concentrations at this station are up to 0.84 nmol/kg lower relative to the dissolved Cr levels at the σ_0 -adjusted SAFe station. The [Cr] deficit is most pronounced at 100 m depth, and shrinks with increasing depth until Cr concentrations at 2T and SAFe coincide at 800 m. Over the depth range of the [Cr] deficit, total measured Cr isotope signatures at 2T are between 0.02‰ and 0.17‰ heavier compared to those of the adjusted SAFe station.

These observations at station 2T are consistent with Cr reduction within the ODZ producing isotopically light, particle-reactive Cr(III), which is partially scavenged by particles and exported to depth. Isotopically heavy Cr(VI) is left behind in the upper water column. The gradual shrinking of the Cr deficit and the heavy isotope anomaly with depth may be caused by: 1) the continuous remineralization of organic matter along with the release of light Cr below the depth of the onset of Cr reduction, and/or 2) the mixing of shallower ODZ water, where Cr reduction peaks, with deeper ODZ water unaffected by Cr reduction.

Station 7T is located closer to the Mexican coast than station 2T. Even though O_2 levels are lower than the Seabird CTD O_2 detection limit (\sim 1.3 μ mol/kg) between 100 m and 800 m depth (Tables 1 and 2), only a slight deficit in total Cr concentrations is observed relative to

the σ_{θ} -adjusted SAFe station (Fig. 6). Likewise, the measured total Cr isotope signatures at station 7T coincide with those seen at SAFe apart from a slightly heavier δ^{53} Cr signature at 600 m.

As this paper was being revised, a paper by Wang et al. (2019) reported data from 11 samples collected at ETNP ODZ stations near ours including some analyses for [Cr(total)], [Cr(III)], [Cr(VI)] and their isotope ratios. We are at a loss to account for differences between their data and ours. They report [Cr] in the upper 300 m ranging from 4.6 to 5.3 nM, where ours range from 2.3–3.1 nM; their δ^{53} Cr(total) values range from 1.36–1.52‰, where ours range from 1.06 to 1.18‰. We believe that our data are correct: (1) we are confident in our methodology, (2) we have reported data for international standard reference seawater (SAFe station, Moos and Boyle, 2019; the GSP reference sample is from the same site), and (3) our Cr upper ocean concentrations are comparable to those of Murray et al. (1983) and Rue et al. (1997).

3.2.2. Santa Barbara Basin

At the time of our sampling, very low oxygen (1.5 μ mol/kg) and nitrate (6.0 μ mol/kg) concentrations and a negative N* = [NO₃⁻] – 16P + 2.90 of –49 μ mol/kg were observed in the bottom waters of the Santa Barbara basin (Fig. 7). Because of the release of phosphate bound to Fe oxyhydroxides under anoxic conditions, this N* somewhat overstates true nitrate loss. As anoxia and denitrification were well established, we can dismiss the potential occurrence of a flushing or turbidity

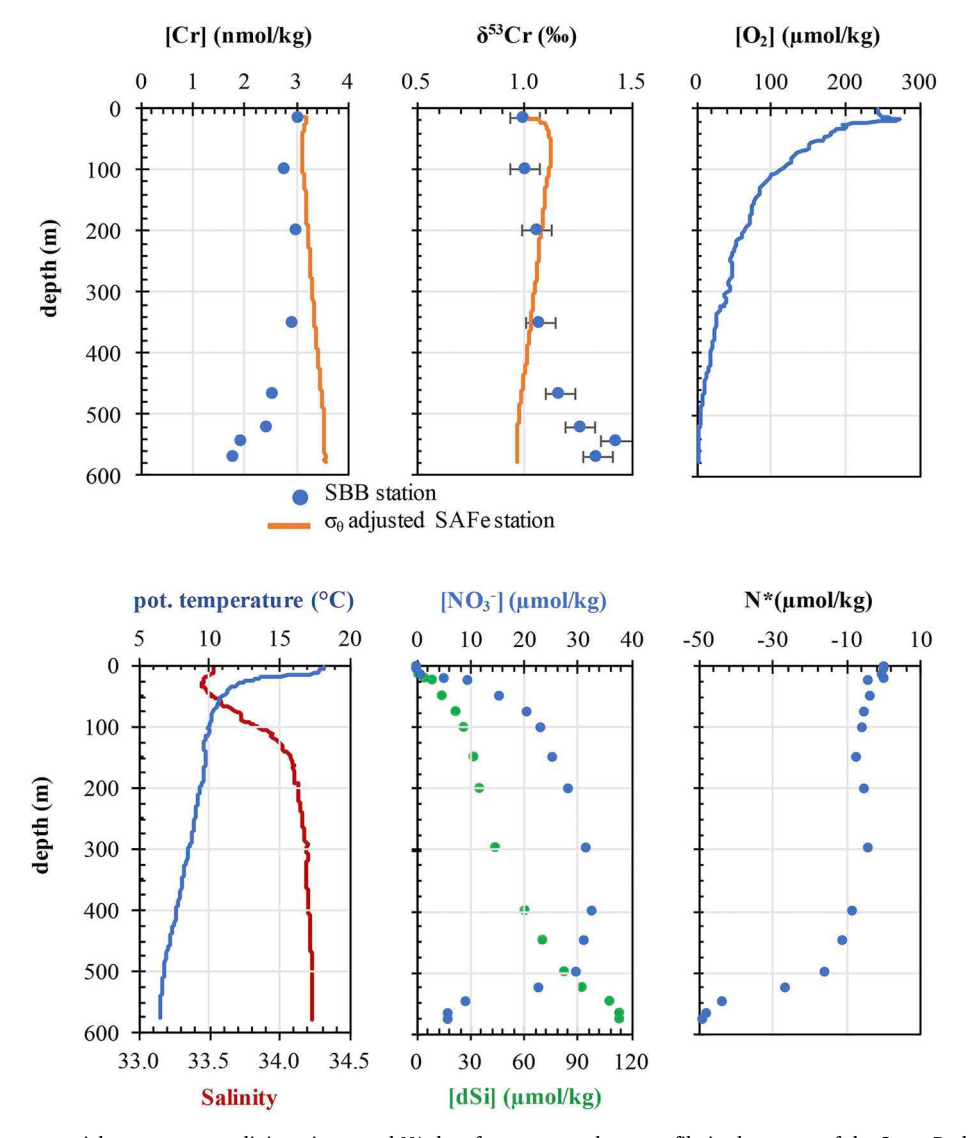


Fig. 7. Chromium, oxygen, potential temperature, salinity, nitrate and N^* data for a water column profile in the center of the Santa Barbara Basin. Note that the depth of the western sill, that connects the Santa Barbara Basin to the North Pacific, is 475 m. Error bars of Cr isotope ratios are 2SD.

current event immediately prior to sampling. Total Cr concentrations were steady over the upper 350 m at $\sim\!3$ nmol/kg except for a minor excursion to 2.78 nmol/kg at 100 m. Over the same depth range, $\delta^{53}\text{Cr}$ isotope signatures increased marginally from +1.00% to +1.07%. Both of these concentration and $\delta^{53}\text{Cr}$ values agree well with our observations of the upper 350 m water column of the adjusted SAFe station ([Cr] = 3.16–3.24 nmol/kg, $\delta^{53}\text{Cr} = +1.01\%$ - +1.11%). At our Santa Barbara Basin site, nitrate concentrations increase in the upper 400 m. The effects of denitrification manifest from 451 m downwards ([O_2] \leq 10.85 µmol/kg) with nitrate concentrations and N* values decreasing. Simultaneously, total Cr concentrations decrease from at least 465 m downwards and reach a minimum concentration of 1.79 nmol/kg at 570 m. Cr isotopic signatures increase from 465 m downwards to a maximum $\delta^{53}\text{Cr}$ value of 1.43% at 545 m.

The Santa Barbara basin data are consistent with Cr reduction under anoxic conditions producing isotopically light, particle-reactive Cr(III). As this Cr(III) fraction is partly exported to depth via particle scavenging, total Cr concentrations drop and isotopically heavy Cr(VI) remains in the bottom waters.

3.2.3. Isotope effect of observed Cr reduction

The fractionation factor (α) , characterizing the observed Cr reduction at station 2T, can be found using the Rayleigh distillation equation

(Rayleigh, 1896; Eqs. (6) and (7)). This equation relates the initial Cr isotope ratio ($\delta^{53}\text{Cr}_0$) and the transient Cr isotope ratio ($\delta^{53}\text{Cr}_t$) of a system to the remaining Cr fraction (f) when Cr is removed with a constant fractionation factor (α).

$$\delta^{53}Cr_t = (\delta^{53}Cr_O + 1000) \times f^{(\alpha - 1)} - 1000$$
(6)

$$f = \frac{C_t}{C_O} \tag{7}$$

The initial Cr isotope ratio and the initial Cr concentration (C_O) can be extracted from the σ -adjusted SAFe profiles at 2T. The measured Cr concentration of seawater samples taken at station 2T serves as the transient Cr concentration (C_t). By choosing reasonable fractionation factors associated with Cr reduction, we can model the Cr isotope ratio of the residual Cr(VI) fraction (Fig. 8). A fractionation factor of $\alpha=0.99956$ ($\epsilon=-0.44\%\pm0.20$, as determined by eye based on Fig. 8) is able to mimic the Cr isotope profile observed at 2T the best. However, it should be noted that as shown by Rue et al. (1997), only a fraction of the light Cr(III) is removed from the water column, and the remaining light Cr(III) partially offsets the residual heavy Cr(VI). So this fractionation factor is the net effect of the reduction and scavenging processes. Also, any suspended particles that have scavenged light Cr (III) will be included in our total dissolvable Cr analysis.

Table 1
Cr isotope ratio and concentration data for stations 2T and 7T in the Eastern Tropical North Pacific Ocean and with a station in the Santa Barbara Basin.

batch no.	location	cruise	station	lat. (°N)	long. (°W)	depth (m)	T (°C)	CTD S (pss)	CTD O ₂ (µmol/kg)	σ_{Φ} (‰)	[Cr] (nmol/kg)	δ ⁵³ Cr (‰)
3	ETNP	NH1410	2T	18.9	108.8	5	27.060	34.904	195.9	22.628	2.78	1.09
						100	14.273	34.668	16.8	25.882	2.27	1.18
						200	11.782	34.747	1.0	26.445	2.66	1.14
						250	11.000	34.685	1.1	26.542	2.72	1.09
						300	10.127	34.622	1.4	26.647	2.73	1.19
						400	8.865	34.583	1.0	26.826	3.07	1.04
						500	7.888	34.568	1.1	26.966	3.21	0.99
						600	6.925	34.541	1.1	27.084	3.36	0.93
						800	5.499	34.534	1.3	27.264	4.01	0.78
4	ETNP	NH1410	7T	18.2	104.2	5	30.262	34.039	189.7	20.917	2.84	1.07
						100	15.284	34.771	1.4	25.742	2.72	1.16
						200	12.717	34.833	1.0	26.331	3.03	1.08
						250	12.231	34.803	1.0	26.405	3.08	1.04
						300	11.760	34.775	1.0	26.474	3.03	1.06
						400	10.390	34.694	1.0	26.661	2.87	1.02
						600	7.448	34.565	1.1	27.029	3.38	1.03
						800	5.919	34.541	1.3	27.218	3.80	0.91
4	Santa	MV1405	29	34.23	120.03	15	16.616	33.509	256.1	24.470	3.06	1.00
	Barbara					100	9.944	33.862	110.5	26.064	2.78	1.00
	Basin					200	9.392	34.142	61.4	26.376	3.00	1.06
						350	8.155	34.204	25.8	26.620	2.94	1.07
						465	7.070	34.234	8.7	26.801	2.55	1.17
						520	6.696	34.245	3.1	26.860	2.42	1.26
						545	6.608	34.247	1.7	26.875	1.96	1.43
						570	6.581	34.247	1.7	26.878	1.79	1.34

Analogous to the Rayleigh distillation calculations of station 2T, we can model the effect of different fractionation factors associated with the observed degree of Cr reduction in the Santa Barbara Basin (Fig. 9). A fractionation factor of $\alpha=0.99935$ ($\epsilon=-0.65\%\pm0.20$, as determined by eye from Fig. 9) is able to recreate the Cr isotope profile observed in the Santa Barbara Basin the best.

3.2.4. Microbial reduction

For several decades, microbes were thought to break down organic matter using electron acceptors in a strict succession dictated by their free energy yields (Froelich et al., 1979). In this traditional view, the dissimilatory usage of electron acceptors with energy yields below that of the $\mathrm{NO_3}^-$ - $\mathrm{NO_2}^-$ couple (such as the $\mathrm{CrO_4}^{2-}$ - $\mathrm{Cr(OH)_2}^+$ and the $\mathrm{SO_4}^{2-}$ - HS $^-$ couple) did not occur until nitrate concentrations were zero. In recent years, metagenomics techniques have revealed that nitrate and sulfate reduction can take place within the same water sample (e.g. Canfield et al., 2010). There is debate over whether the reductions are occurring homogeneously or if sulfate reduction is occurring in small microenvironments within the larger sample (Bianchi et al., 2018). Since chromate's reduction potential at seawater pH is only slightly lower than that of nitrate and higher than that of sulfate (Stumm and Morgan, 2012), it is conceivable that microbes directly reduce chromate in oxygen depleted waters.

The microbial reduction of nitrate leaves the residual NO_3^- enriched in ^{15}N , which results in an apparent isotope effect of 20%-30% (e.g. Cline and Kaplan, 1975; Brandes et al., 1998; Voss et al., 2001; Sutka et al., 2004). Compared to typical deep-sea $\delta^{15}N_{NO3}$. signatures (+5.5%; Casciotti, 2016), all $\delta^{15}N_{NO3}$. signatures recorded at station 2T are heavy (Fig. 5), which indicates heterotrophic denitrification. When $\delta^{15}N_{NO3}$. signatures are plotted against δ^{53} Cr signatures at station 2T (Fig. 10), a strong correlation is observed. Excluding a single data point at 100 m, $R^2=0.91$ (without exclusion: $R^2=0.58$). This strong correlation between $\delta^{15}N_{NO3}$. and δ^{53} Cr signatures implies that Cr cycling in ODZs (like N cycling; Cline & Kaplan, 1975; Altabet et al., 1995; Voss et al., 2001; Ward et al., 2009) may be driven by sinking-flux dependent microbial activity.

Although the isotopic signature of ${\rm NO_3}^-$ was not determined during our occupation of the Santa Barbara Basin station, the observed Cr reduction signal aligns well with the bottom water's negative N*

excursion, which is another indicator of denitrification. Additionally, an earlier occupation of the basin by Sigman et al. (2003) revealed a significant shift to heavier $\delta^{15} N$ of NO_3^- values within the anoxic layer (~8.5% at 500 m vs. ~12% at the basin's bottom depth), which was interpreted as a denitrification signal. Therefore, the Cr reduction signal that we observe in the Santa Barbara Basin's bottom water may at least partially be a product of direct microbial Cr reduction in the water column.

3.3. Cr reduction via Fe(II)

Alternatively to or in conjunction with direct microbial Cr reduction, dissolved Fe(II) (dFe(II)) may have acted as a reductant of Cr(VI) (Eary and Rai, 1988; Sedlack and Chan, 1997) at both station 2T and within the Santa Barbara Basin. Previously, low oxygen shelf waters off of Oregon and Washington have been observed to be sources of dFe(II) to the coastal upwelling region (Lohan and Bruland, 2008). Similarly, reducing continental-margin sediments were observed to be the source of dFe(II) to Peruvian offshore waters (Chever et al., 2015; Hong and Kester, 1986). Based on these findings, it is conceivable that Fe(II) was produced in the anoxic pore waters of the Mexican shelf and subsequently transported offshore to station 2T. However, if dFe(II) originating from reducing continental-margin sediments was responsible for Cr(VI) reduction at station 2T, we would have expected to see the same or a higher extent of Cr reduction at station 7T as it is located closer to the Mexican coast. Furthermore, in-situ reduction of Fe in the ODZ cannot be excluded. Even though no direct dFe(II) measurements have been reported for the ODZ of the ETNP, total Fe concentrations have been shown to be unusually high here (up to 6 nmol/kg at 150 m, 18°N 108°W, Landing and Bruland, 1987) and Fe(II) is likely to make up an significant fraction of total Fe (Moffett et al., 2007).

When anoxia is firmly established within the bottom waters of the Santa Barbara Basin, high dFe(II) levels likely persist in both the bottom waters and the sediments. John et al. (2012) saw total Fe concentrations increase from 8.8 nmol/kg above sill depth to 29.5 nmol/kg at 570 m depth within the basin's anoxic bottom waters. Simultaneously, Fe isotope signatures (δ^{56} Fe) shifted to much lighter values within the bottom waters, which are typically produced by Fe(III) reduction to Fe (II). John et al. (2012) ascribed their observations to Fe reduction in the

Table 2 Nitrate $\delta^{15}N$ and concentration data for stations 2T and 7T in the Eastern Tropical North Pacific.

location	cruise	station	lat. (°N)	long. (°W)	depth (m)	T (°C)	CTD S (pss)	CTD O ₂ (µmol/kg)	NO ₃ ⁻ (μmol/kg)	DIP (μmol/kg)	$NO_3^- \delta^{15}N$ (‰
ETNP	NH1410	2T	18.90	108.80	81	16.469	34.441	70.9	19.0		9.33
					101	15.330	34.623	34.1	24.0		12.40
					125	14.159	34.675	13.9	25.9		13.74
					151	13.076	34.746	1.5	26.3		14.77
					199	12.037	34.761	1.1	23.8		22.21
					249	11.333	34.721	1.1	25.3		18.73
					302	10.391	34.636	1.9	29.2		19.78
					400	8.943	34.590	1.0	31.1		15.74
					500	7.901	34.569	0.9	29.1		14.11
					600	6.963	34.544	1.2	33.3		10.60
					700	6.214	34.535	1.1	39.5		9.06
					800	5.519	34.534	1.2	43.8		7.89
					902	5.076	34.536	2.6	40.9		7.10
					1000	4.601	34.538	6.6	39.7		6.77
					1199	3.881	34.561	19.2	43.9		6.39
					1302	3.567	34.573	27.1	43.8		6.08
					1401	3.325	34.583	34.2	44.1		5.85
					1501	3.066	34.593	42.3	39.5		5.55
					1602	2.880	34.602	49.3	39.7		5.57
					1695	2.683	34.612	57.2	39.2		5.66
					1800	2.425	34.623	67.7	45.6		5.19
					1901	2.285	34.632	75.3	44.7		5.33
					1999	2.150	34.639	82.1	44.3		5.09
					2200	2.007	34.649	90.6	40.2		5.09
					2301	1.930	34.653	94.7	43.8		5.00
ETNP	NH1410	7T	18.20	104.20	56	19.508	34.548	93.7	26.6	2.68	14.24
					60	19.467	34.570	54.4	22.8	2.16	8.89
					77	17.886	34.616	19.3	26.5	2.18	8.32
					85	17.206	34.659	13.1	28.1	2.21	8.43
					91	16.658	34.692	8.1	28.7	2.46	8.39
					99	16.035	34.732	1.0	26.4	2.55	10.19
					100	14.137	34.771	0.9	27.9	2.61	13.41
					113	14.614	34.802	1.0	24.1	2.59	12.88
					201	12.032	34.787	1.0	29.0	2.48	11.22
					299	11.864	34.785	1.1	27.1	2.73	13.63
					300	11.034	34.727	1.0	28.8	2.58	12.01
					398	10.411	34.697	1.0	23.7	2.90	20.90
					501	8.935	34.621	0.8	27.0	3.33	19.23
					601	7.444	34.566	1.1	33.5	3.36	13.57
					705	6.459	34.547	1.2	39.1	3.60	9.85
					801	5.917	34.542	1.2	42.2	3.81	8.67
					891	5.313	34.532	1.9	43.4	3.45	8.00
					998	4.762	34.537	5.1	44.0	3.75	7.07
					770	7.702	JT.JJ/	U.1	17.0	3.73	/.0/

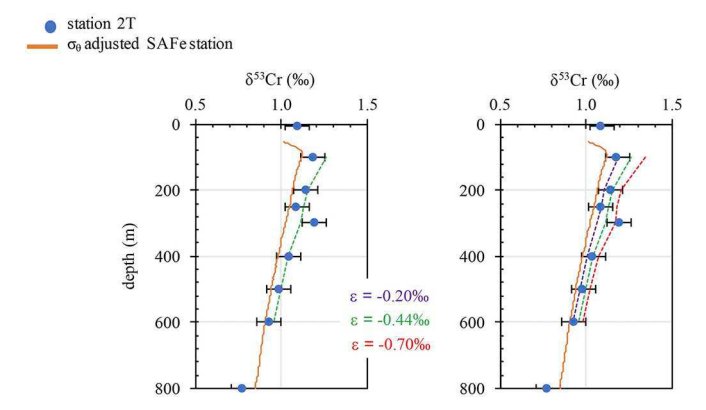


Fig. 8. Using the Rayleigh distillation equation, we model the Cr isotope ratio of the residual Cr(VI) fraction after Cr reduction. For this purpose, three fractionation factors have been chosen. The fractionation factor shown in green is the best fit to the observed profiles at station 2T. (For interpretation of the references to colour in this figure legend, the reader is referred to the web version of this article.)

anoxic sediment pore waters and a subsequent flux of Fe(II) into the bottom waters. At the time our Cr profile was taken, total dFe concentrations exceeded 50 nmol/kg at 573 m depth (Boiteau et al., 2019)

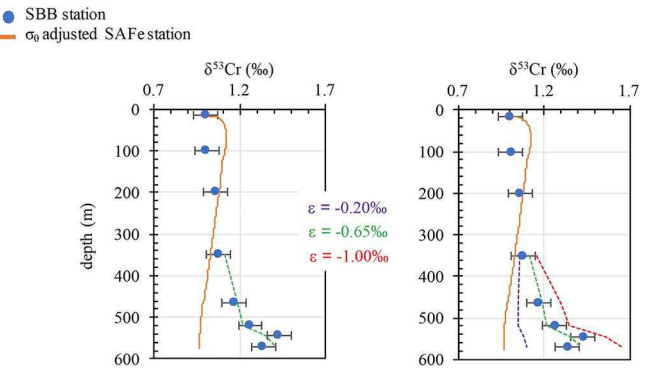


Fig. 9. Using the Rayleigh distillation equation, we model the Cr isotope ratio of the residual Cr(VI) fraction after Cr reduction. For this purpose, three fractionation factors have been chosen. The fractionation factor shown in green is the best fit to our Santa Barbara Basin data. (For interpretation of the references to colour in this figure legend, the reader is referred to the web version of this article.)

with dFe(II) likely accounting for the majority of it. In consequence, dFe (II) is a potential reductant of Cr(VI) in the bottom water of the Santa Barbara Basin.

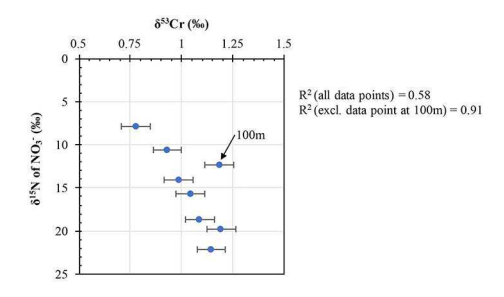


Fig. 10. $\delta^{15} N_{NO3\text{-}}$ signatures of station 2T vs. $\delta^{53} \text{Cr}$ signatures of station 2T.

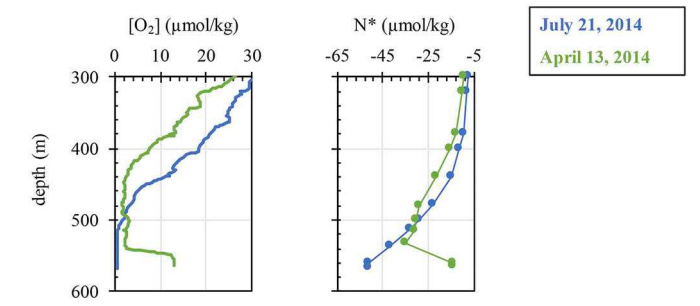


Fig. 11. Oxygen concentrations and N^* data measured in the Santa Barbara Basin in April and July 2014 are shown. Oxygen and nutrient data, which were used to calculate N^* , originate from quarterly expeditions conducted by the California Cooperative Oceanic Fisheries Investigations (CalCOFI).

3.4. Sedimentary Cr reduction

As of yet we have only discussed scenarios in which the reduction of Cr occurs in the water column. While this may be appropriate for the oxygen deficient zone of the ETNP, it is possible that Cr reduction in the Santa Barbara Basin could occur in the anoxic sediment porewaters.

If Cr reduction is indeed happening in the anoxic pore waters of the sediment, we would expect a steep Cr concentration gradient near the sediment-water interface. This would result in the transfer of Cr from the bottom waters into the sediments, which in turn lowers Cr concentrations in these bottom waters. Such a steep concentration gradient is known to occur for nitrate in the upper pore waters of reducing sediments, and evidence suggests that total diffusion of nitrate into the sedimentary denitrification zone produces a relatively minor nitrate δ^{15} N fractionation (\sim 1.5‰) because of diffusion limitation (Brandes and Devol, 1997, 2002). In the absence of contrary information, we should expect a similarly minor isotope fractionation for sedimentary Cr reduction. Hence, although sedimentary Cr reduction is a plausible mechanism for reducing bottom water chromium

concentrations and enriching the Cr concentration of reducing sediments, it would not appear to be a viable mechanism for the heavy Cr isotope enrichments that we observe in the bottom waters of the Santa Barbara Basin.

Nevertheless, potential sedimentary Cr reduction mechanisms would largely mirror the water column ones: (1) Taking advantage of the different N isotope effects, that water column and sedimentary denitrification produce in the remaining NO₃⁻, Sigman et al. (2003) attributed at least 76% of the observed nitrate loss within the Santa Barbara Basin to sedimentary denitrification. Given chromate's and nitrate's similar reduction potential at seawater pH, it is conceivable that microbial reduction of chromate (like nitrate) occurs in both the anoxic bottom water and in the anoxic sediment porewaters. (2) As previously discussed, an Fe isotope study of the Santa Barbara Basin by John et al. (2012) indicated that Fe(II) is produced in the anoxic sediment pore waters. Fe(II) may therefore reduce chromium in both the anoxic bottom waters and in the sediment pore waters of the Santa Barbara Basin. (3) Furthermore, Cr may be reduced by acid volatile sulfides in the anoxic sediment pore waters (Graham and Bouwer, 2010).

To assess the feasibility of future Cr porewater studies, we estimate the depth horizon over which porewater Cr would become consumed, if all the Cr reduction occurred in the anoxic sediments. Under this assumption, a porewater Cr concentration gradient can be calculated using Fick's first law of diffusion (Fick, 1855). Applying this law, the Cr removal flux over the Santa Barbara Basin's anoxic sediment area should equal the diffusion coefficient (D) multiplied by the pore water Cr concentration gradient ($\Delta [Cr]/\Delta z$) (Eq. (8)). In order to calculate the Cr removal flux over the basin's anoxic sediment area, we need to estimate how much total Cr is lost in the basin, and the time since the basin's bottom waters were last renewed (Eq. (9)).

Cr removal flux over the SBB's anoxic sediment area =
$$D \times \frac{\Delta [Cr]}{\Delta z}$$
 (8)

total Cr lost in SBB

anoxic sediment area of SBB × time since last renewal of bottom waters $= D \times \frac{\Delta \ [Cr]}{\Delta \ z}$

(9

We roughly integrate the Cr lost in the basin by placing a triangle in the space between the Cr concentration profile of the adjusted SAFe station and that of our basin site (= $0.5 \times \left(3.00 \, \frac{nmol \, Cr}{kg} - 1.79 \, \frac{nmol \, Cr}{kg}\right) \times (585m - 465m)$) and multiplying it by the basin's anoxic sediment area. As this latter term appears in the denominator, the terms will cancel out.

On a quarterly basis, oxygen and nutrient concentrations in the water column of the Santa Barbara Basin are determined by the California Cooperative Oceanic Fisheries Investigations (CalCOFI). One CalCOFI

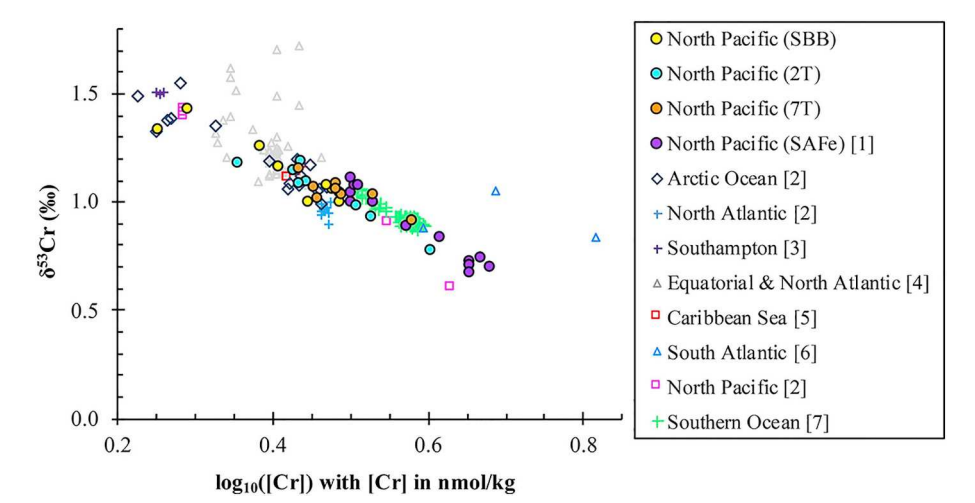


Fig. 12. Data from stations 2T, 7T and Santa Barbara Basin site are plotted in δ⁵³Cr-log[Cr]) space alongside published seawater Cr isotope data: [1] Moos and Boyle (2019); [2] Scheiderich et al. (2015); [3] Bonnand et al. (2013); [4] Goring-Harford et al. (2018); [5] Holmden et al. (2016); [6] Pereira et al. (2016); [7] Rickli et al. (2019).

occupation took place three days before our samples were taken and confirms that anoxia and denitrification were well–established in the bottom waters immediately prior to our sampling (Fig. 11). In contrast, CalCOFI data from April 13th, 2014 show higher $\rm O_2$ levels (up to 13 μ mol/kg) and nitrate concentrations are not substantially depleted relative to phosphate concentrations (Fig. 11). After a major flushing event, it takes \sim 2 months for anoxia and denitrification to manifest in the basin's bottom water (Sholkovitz and Gieskes, 1971). In consequence, the bottom waters of the Santa Barbara Basin were at least partially replaced sometime between mid-February and mid-April 2014. For our calculations, we estimate that the last renewal of the bottom waters occurred 4 months prior to sampling, which took place on July 24, 2014.

Using these estimates and a typical sediment diffusion coefficient of $2.5 \times 10^{-6} \frac{cm^2}{s}$, we arrive at a pore water Cr concentration gradient of $\sim 280 \, \frac{nM}{cm}$. Given that the bottom waters only hold 1.84 nM of Cr, Cr in sediment pore waters would get exhausted over ~ 0.07 mm. This narrow depth range would make any Cr analysis in Santa Barbara Basin porewaters extremely challenging.

4. Conclusions

Our observations at station 2T in the ETNP and at our Santa Barbara Basin site are consistent with Cr reduction in anoxic waters producing isotopically light, particle-reactive Cr(III), which is partially scavenged by particles and exported to depth. Isotopically heavy Cr(VI) is left behind in the upper water column. Since seawater samples from station 2T were not filtered, the magnitude of the Cr reduction signal may have been suppressed by the presence of isotopically light Cr(III) particles. Surprisingly, the isotope data of our three partly anoxic sites fall on the "global" δ^{53} Cr-log[Cr] line seen in oxic ocean water (Fig. 12). Since the "global" oxic relationship is attributed to biological uptake and regeneration from sinking biogenic particles, it would appear that the net ETNP ODZ total Cr isotope fractionation coincidentally yields the same value as that for the biological fractionation. We will show elsewhere that this coincidence in the ETNP is a result of a higher Cr isotope fractionation during reduction balanced by the retention of some of the light Cr(III) within the water column.

The observed correlation of δ^{53} Cr and $\delta^{15}N_{NO3}$ at station 2T suggests that Cr reduction may be microbially mediated. Alternatively, Cr (VI) may be reduced by Fe(II), which was generated in-situ by dissimilatory Fe reduction and/or was generated in the anoxic pore waters of the Mexican shelf by dissimilatory Fe reduction and subsequently transported offshore to station 2T. In the Santa Barbara Basin, Cr reduction may take place via the same mechanisms in the anoxic bottom waters and/or in the anoxic sediment pore waters. Additionally, acid volatile sulfides may contribute to Cr(VI) reduction in the anoxic sediment pore waters. Although the sedimentary Cr reduction can contribute to lowering the Cr concentration of the bottom waters, it is unlikely to result in significant Cr isotope fractionation. If all of the observed Cr reduction took place in the basin's sediment, Cr in the pore waters would get depleted over a depth range of less than a millimeter. This narrow depth range would make any Cr analysis in such pore waters extremely challenging.

In our discussion we used the SAFe station as an oxygen-bearing water column counterpart. Above 500 m – equivalent to the upper 2/3 of the ETNP ODZ – SAFe has >100 μ mol/kg O_2 . While it is our best possible comparison choice among the published marine Cr isotope profiles, its use should come with a caveat. The peak in heavy Cr and a subtle decrease in Cr concentrations at SAFe (at 200 m depth) are located along the same isopycnal as the biggest total Cr deficit and heaviest Cr anomaly at station 2T (at 100 m depth). This point is best illustrated by comparing the Cr profiles of 2T and the σ_{θ} adjusted SAFe station at 100 m (Fig. 5). It is conceivable that a signal of Cr reduction (=lower [Cr], heavier δ^{53} Cr) generated within the ODZ of the ETNP at station 2T can advect or mix out to the SAFe station. In that case, a direct comparison between the two stations may underestimate the magnitude of Cr reduction and removal

occurring within the ODZ. To verify this hypothesis, a transect from the ODZ further into oxic waters of the North Pacific is required. Alternatively, a more remote station in the North Pacific such as Station ALOHA (22.75° N, 158°W) could be analyzed with the hope that it is less impacted by transport of a Cr reduction signal out of the ODZ.

Contributors

S.B. Moos processed the samples, made the Cr isotope measurements, wrote the first draft and participated in its revisions, and prepared the figures. E.A. Boyle assisted with the Cr isotope measurements, handled the manuscript revision, and assembled the data tables. M. Altabet and A. Bourbonnais collected the samples, measured the nitrogen isotopes, and participated in manuscript revisions.

Declaration of Competing Interest

The authors have no competing interests.

Acknowledgements

We thank Frank Stewart for his contributions on the NH1410 ETNP cruise and Jessica Fitzsimmons for collecting the MV1405 Santa Barbara Basin samples. We thank the members of SBM's Ph.D. thesis committee (Sune Nielsen, Colleen Hansel) for discussions and suggestions during the course of her research. The filtered Cr concentration data at station P2 (RR18-04) were kindly provided by Tianyi Huang. Nutrient data for the Santa Barbara Basin were kindly provided by Tyler Coale and Kenneth Bruland. Rick Kayser assisted with laboratory and instrument maintenance and acid purification. We thank the officers and crews of the R/V New Horizon and R/V Melville for their efforts on our behalf. This research was supported by US National Science Foundation Grants (NSF OCE-0926197, OCE-1233749, OCE-1357224), the Singapore National Research Foundation through the Singapore-MIT Alliance for Research and Technology (Award No. WBS 6916070), and the Center for Microbial Research and Education (NSF-OIA Award No. EF-0424599), and a MIT-WHOI Joint Program Science Fellowship.

References

- Altabet, M.A., Francois, R., Murray, D.W., Prell, W.L., 1995. Climate-related variations in denitrification in the Arabian Sea from sediment 15N/14N ratios. Nature 373, 506–509. Ball, J.W., Bassett, R.L., 2000. Ion exchange separation of chromium from natural water
- Ball, J.W., Bassett, R.L., 2000. Ion exchange separation of chromium from natural wate matrix for stable isotope mass spectrometric analysis. Chem. Geol. 168, 123–134. https://doi.org/10.1016/S0009-2541(00)00189-3.
- Basu, A., Johnson, T.M., 2012. Determination of hexavalent chromium reduction using Cr stable isotopes: isotopic fractionation factors for permeable reactive barrier materials. Environ. Sci. Technol. 46, 5353–5360. https://doi.org/10.1021/es204086y.
- Berna, E.C., Johnson, T.M., Makdisi, R.S., Basti, A., 2010. Cr stable isotopes as indicators of Cr(VI) reduction in groundwater: a detailed time-series study of a point-source plume. Environ. Sci. Technol. 44, 1043–1048. https://doi.org/10.1021/es902280s.
- Bianchi, D., Weber, T.S., Kiko, R., Deutsch, C., 2018. Global niche of marine anaerobic metabolisms expanded by particle microenvironments. Nature Geosci. 11, 263–268.
- Boiteau, R.M., Till, C.P., Coale, T.H., Fitzsimmons, J.N., Bruland, K.W., Repeta, D.J., 2019. Patterns of iron and siderophore distributions across the California Current System. Limnol. Oceanogr. 64, 376–389. https://doi.org/10.1002/lno.11046.
- Bonnand, P., Parkinson, I.J., James, R.H., Karjalainen, A.-M., Fehr, M.A., 2011. Accurate and precise determination of stable Cr isotope compositions in carbonates by double spike MC-ICP-MS. J. Anal. At. Spectrom. 26, 528–535.
- Bonnand, P., James, R.H., Parkinson, I.J., Connelly, D.P., Fairchild, I.J., 2013. The chromium isotopic composition of seawater and marine carbonates. Earth Planet. Sci. Lett. 382, 10–20. https://doi.org/10.1016/j.epsl.2013.09.001.
- Brandes, J.A., Devol, A.H., 1997. Isotopic fractionation of oxygen and nitrogen in coastal marine sediments. Geochim. Cosmochim. Acta 61, 1793–1801. https://doi.org/10. 1016/S0016-7037(97)00041-0.
- Brandes, J.A., Devol, A.H., 2002. A global marine-fixed nitrogen isotopic budget: implications for Holocene nitrogen cycling. Glob. Biogeochem. Cycles 16https://doi.org/10.1029/2001GB001856. 67-1-67-14.
- Brandes, J.A., Devol, A.H., Yoshinari, T., Jayakumar, D.A., Naqvi, S.W.A., 1998. Isotopic composition of nitrate in the central Arabian Sea and eastern tropical North Pacific: a tracer for mixing and nitrogen cycles. Limnol. Oceanogr. 43, 1680–1689. https://doi.org/10.4319/lo.1998.43.7.1680.
- Brandt, P., Bange, H.W., Banyte, D., Dengler, M., Didwischus, S.-H., Fischer, T.,

- Greatbatch, R.J., Hahn, J., Kanzow, T., Karstensen, J., Körtzinger, A., Krahmann, G., Schmidtko, S., Stramma, L., Tanhua, T., Visbeck, M., 2015. On the role of circulation and mixing in the ventilation of oxygen minimum zones with a focus on the eastern tropical North Atlantic. Biogeosciences 12, 489–512. https://doi.org/10.5194/bg-12-489-2015.
- Canfield, D.E., Stewart, F.J., Thamdrup, B., De Brabandere, L., Dalsgaard, T., Delong, E.F., Revsbech, N.P., Ulloa, O., 2010. A cryptic sulfur cycle in oxygen-minimum-zone waters off the Chilean coast. Science 330 (80), 1375–1378. https://doi.org/10.1126/ science.1196889.
- Casciotti, K.L., 2016. Nitrogen and oxygen isotopic studies of the marine nitrogen cycle. Annu. Rev. Mar. Sci. 8, 379–407. https://doi.org/10.1146/annurev-marine-010213-135052
- Chever, F., Rouxel, O.J., Croot, P.L., Ponzevera, E., Wuttig, K., Auro, M., 2015. Total dissolvable and dissolved iron isotopes in the water column of the Peru upwelling regime. Geochim. Cosmochim. Acta 162, 66–82. https://doi.org/10.1016/j.gca.2015. 04.021
- Cline, J.D., Kaplan, I.R., 1975. Isotopic fractionation of dissolved nitrate during denitrification in the eastern tropical north pacific ocean. Mar. Chem. 3, 271–299. https://doi.org/10.1016/0304-4203(75)90009-2.
- Døssing, L.N., Dideriksen, K., Stipp, S.L.S., Frei, R., 2011. Reduction of hexavalent chromium by ferrous iron: A process of chromium isotope fractionation and its relevance to natural environments. Chem. Geol. 285, 157–166. https://doi.org/10. 1016/j.chemgeo.2011.04.005.
- Eary, L.E., Rai, D., 1987. Kinetics of chromium (III) oxidation to chromium (VI) by reaction with manganese dioxide. Environ. Sci. Technol. 21, 1187–1193.
- Eary, L.E., Rai, D., 1988. Chromate removal from aqueous wastes by reduction with ferrous ion. Environ. Sci. Technol. 22, 972–977.
- Ellis, A.S., Johnson, T.M., Bullen, T.D., 2002. Chromium isotopes and the fate of hexavalent chromium in the environment. Science 295 (80), 2060–2062.
- Emerson, S., Cranston, R.E., Liss, P.S., 1979. Redox species in a reducing fjord: equilibrium and kinetic considerations. Deep Sea Res. Part A.Oceanographic Res. Pap. 26, 859–878. https://doi.org/10.1016/0198-0149(79)90101-8.
- Fick, A., 1855. V. On liquid diffusion. Philos. Mag. 10, 30–39. https://doi.org/10.1080/ 14786445508641925.
- Fine, R.A., Maillet, K.A., Sullivan, K.F., Willey, D., 2001. Circulation and ventilation flux of the Pacific Ocean. J. Geophys. Res. 106, 22159–22178.
- Froelich, P.N., Klinkhammer, G.P., Bender, M.L., Luedtke, N.A., Heath, G.R., Cullen, D., Dauphin, P., Hammond, D., Hartman, B., Maynard, V., 1979. Early oxidation of organic matter in pelagic sediments of the eastern equatorial Atlantic: suboxic diagenesis. Geochim. Cosmochim. Acta 43, 1075–1090. https://doi.org/10.1016/0016-7037(79)90095-4.
- Garcia, H.E., Locarnini, R.A., Boyer, T.P., Antonov, J.I., Baranova, O.K., Zweng, M.M., Johnson, D.R., 2010. World Ocean atlas 2009, volume 3: Dissolved oxygen, apparent oxygen utilization, and oxygen saturation. In: Levitus, S. (Ed.), NOAA Atlas NESDIS 70. U.S. Government Printing Office, Washington, D.C., pp. 344.
 Goring-Harford, H.J., Klar, J.K., Pearce, C.R., Connelly, D.P., Achterberg, E.P., James,
- Goring-Harford, H.J., Klar, J.K., Pearce, C.R., Connelly, D.P., Achterberg, E.P., James, R.H., 2018. Behaviour of chromium isotopes in the eastern sub-tropical Atlantic oxygen minimum zone. Geochim. Cosmochim. Acta 236, 41–59. https://doi.org/10.1016/J.GCA.2018.03.004.
- Götz, A., Heumann, K.G., 1988. Chromium trace determination in inorganic, organic and aqueous samples with isotope dilution mass spectrometry. Fresenius' Z. Anal. Chem. 331, 123–128.
- Graham, A.M., Bouwer, E.J., 2010. Rates of hexavalent chromium reduction in anoxic estuarine sediments: pH effects and the role of acid volatile sulfides. Environ. Sci. Technol. 44, 136–142. https://doi.org/10.1021/es9013882.
- Holmden, C., Jacobson, A.D., Sageman, B.B., Hurtgen, M.T., 2016. Response of the Cr isotope proxy to Cretaceous Ocean Anoxic Event 2 in a pelagic carbonate succession from the Western Interior Seaway. Geochim. Cosmochim. Acta 186, 277–295.
- Hong, H., Kester, D.R., 1986. Redox state of iron in the offshore waters of Peru1. Limnol. Oceanogr. 31, 612–626. https://doi.org/10.4319/lo.1986.31.3.0612.
- Izbicki, J.A., Bullen, T.D., Martin, P., Schroth, B., 2012. Delta Chromium-53/52 isotopic composition of native and contaminated groundwater, Mojave Desert. USA. Appl. Geochemistry 27, 841–853. https://doi.org/10.1016/j.apgeochem.2011.12.019.
- John, S.G., Mendez, J., Moffett, J., Adkins, J., 2012. The flux of iron and iron isotopes from San Pedro Basin sediments. Geochim. Cosmochim. Acta 93, 14–29. https://doi. org/10.1016/j.gca.2012.06.003.
- Kieber, R.J., Helz, G.R., 1992. Indirect photoreduction of aqueous chromium(VI). Environ. Sci. Technol. 26, 307–312.
- Kitchen, J.W., Johnson, T.M., Bullen, T.D., Zhu, J., Raddatz, A., 2012. Chromium isotope fractionation factors for reduction of Cr(VI) by aqueous Fe(II) and organic molecules. Geochim. Cosmochim. Acta 89, 190–201. https://doi.org/10.1016/j.gca.2012.04.049.
- Landing, W.M., Bruland, K.W., 1987. The contrasting biogeochemistry of iron and manganese in the Pacific Ocean. Geochim. Cosmochim. Acta 51, 29–43. https://doi.org/10.1016/0016-7037(87)90004-4.
- Lohan, M.C., Bruland, K.W., 2008. Elevated Fe(II) and dissolved Fe in hypoxic shelf waters off Oregon and Washington: an enhanced source of Iron to coastal upwelling regimes. Environ. Sci. Technol. 42, 6462–6468. https://doi.org/10.1021/es800144j.
- Lovley, D.R., 1993. Dissimilatory metal reduction. Annu. Rev. Microbiol. 47, 263–290.
 Luyten, J.R., Pedlosky, J., Stommel, H., 1983. The ventilated thermocline. J. Phys.
 Oceanogr. 13, 292–309.

- McIlvin, M.R., Altabet, M.A., 2005. Chemical conversion of nitrate and nitrite to nitrous oxide for nitrogen and oxygen isotopic analysis in freshwater and seawater. Anal. Chem. 77, 5589–5595. https://doi.org/10.1021/AC050528S.
- Moffett, J.W., Goepfert, T.J., Naqvi, S.W.A., 2007. Reduced iron associated with secondary nitrite maxima in the Arabian Sea. Deep Sea Res. Part I Oceanogr. Res. Pap. 54, 1341–1349. https://doi.org/10.1016/j.dsr.2007.04.004.
- Moos, S.B., Boyle, E.A., 2019. Determination of accurate and precise chromium isotope ratios in seawater samples by MC-ICP-MS illustrated by analysis of SAFe Station in the North Pacific Ocean. Chem. Geol. 511, 481–493. https://doi.org/10.1016/J. CHEMGEO.2018.07.027.
- Murray, J.W., Spell, B., Paul, B., 1983. The contrasting geochemistry of manganese and chromium in the Eastern Tropical Pacific Ocean. In: Wong, C.S., Boyle, E., Bruland, K.W., Burton, J.D., Goldberg, E.D. (Eds.), Trace Metals in Sea Water, NATO Conference Series. Springer, US, pp. 643–669. https://doi.org/10.1007/978-1-4757-6864-0_37.
- Palme, H., 1920. Studien über die Zersetzung der Überschwefelsäure. Z. Anorg. Allg. Chem. 112, 97–130. https://doi.org/10.1002/zaac.19201120105.
- Pereira, N.S., Voegelin, A.R., Paulukat, C., Sial, A.N., Ferreira, V.P., Frei, R., 2016. Chromium-isotope signatures in scleractinian corals from the Rocas atoll, tropical South Atlantic. Geobiology 14, 54–67. https://doi.org/10.1111/gbi.12155.
- Pettine, M., Millero, F.J., 1990. Chromium speciation in seawater: the probable role of hydrogen peroxide. Limnol. Oceanogr. 35, 730–736.
- Pettine, M., Millero, F.J., Passino, R., 1994. Reduction of chromium (VI) with hydrogen sulfide in NaCl media. Mar. Chem. 46, 335–344.
- Pettine, M., D'Ottone, L., Campanella, L., Millero, F.J., Passino, R., 1998. The reduction of chromium (VI) by iron (II) in aqueous solutions. Geochim. Cosmochim. Acta 62, 1509–1519. https://doi.org/10.1016/S0016-7037(98)00086-6.
- Rai, D., Eary, L.E., Zachara, J.M., 1989. Environmental chemistry of chromium. Sci. Total Environ. 86, 15–23.
- Rayleigh, Lord, 1896. L. Theoretical considerations respecting the separation of gases by diffusion and similar processes. London, Edinburgh, Dublin Philos. Mag. J. Sci. 42, 493–498.
- Rickli, J., Janssen, D.J., Hassler, C., Ellwood, M.J., Jaccard, S.L., 2019. Chromium biogeochemistry and stable isotope distribution in the Southern Ocean. Geochim. Cosmochim. Acta 262, 188–206. https://doi.org/10.1016/J.GCA.2019.07.033.
- Rudge, J.F., Reynolds, B.C., Bourdon, B., 2009. The double spike toolbox. Chem. Geol. 265, 420–431. https://doi.org/10.1016/j.chemgeo.2009.05.010.
- Rue, E.L., Smith, G.J., Cutter, G.A., Bruland, K.W., 1997. The response of trace element redox couples to suboxic conditions in the water column. Deep Sea Res. Part I Oceanogr. Res. Pap. 44, 113–134. https://doi.org/10.1016/S0967-0637(96)00088-X.
- Scheiderich, K., Amini, M., Holmden, C., Francois, R., 2015. Global variability of chromium isotopes in seawater demonstrated by Pacific, Atlantic, and Arctic Ocean samples. Earth Planet. Sci. Lett. 423, 87–97. https://doi.org/10.1016/j.epsl.2015.04.030.
- Schlitzer, R., 2013. Ocean Data View.
- Schroeder, D.C., Lee, G.F., 1975. Potential transformations of chromium in natural waters. Water Air Soil Pollut. 4, 355–365.
- Sedlack, D.L., Chan, P.G., 1997. Reduction of hexavalent chromium by ferrous iron. Geochim. Cosmochim. Acta 61, 2185–2192.
- Semeniuk, D.M., Maldonado, M.T., Jaccard, S.L., 2016. Chromium uptake and adsorption in marine phytoplankton – implications for the marine chromium cycle. Geochim. Cosmochim. Acta 184, 41–54. https://doi.org/10.1016/j.gca.2016.04.021.
- Sholkovitz, E.R., Gieskes, J.M., 1971. A physical-chemical study of the flushing of the Santa Barbara Basin. Limnol. Oceanogr. 16, 479–489. https://doi.org/10.4319/lo. 1971.16.3.0479.
- Sigman, D.M., Robinson, R., Knapp, A.N., van Geen, A., McCorkle, D.C., Brandes, J.A., Thunell, R.C., 2003. Distinguishing between water column and sedimentary denitrification in the Santa Barbara Basin using the stable isotopes of nitrate. Geochem. Geophys. Geosyst. 4https://doi.org/10.1029/2002GC000384. n/a-n/a.
- Sikora, E.R., Johnson, T.M., Bullen, T.D., 2008. Microbial mass-dependent fractionation of chromium isotopes. Geochim. Cosmochim. Acta 72, 3631–3641. https://doi.org/ 10.1016/j.gca.2008.05.051.
- Stumm, W., Morgan, J.J., 2012. Aquatic Chemistry: Chemical Equilibria and Rates in Natural Waters. 126 John Wiley & Sons.
- Sutka, R.L., Ostrom, N.E., Ostrom, P.H., Phanikumar, M.S., 2004. Stable nitrogen isotope dynamics of dissolved nitrate in a transect from the North Pacific subtropical gyre to the eastern tropical North Pacific. Geochim. Cosmochim. Acta 68, 517–527. https:// doi.org/10.1016/S0016-7037(03)00483-6.
- Van der Weijden, C.H., Reith, M., 1982. Chromium (III)—chromium (VI) interconversions in seawater. Mar. Chem. 11, 565–572.
- Voss, M., Dippner, J.W., Montoya, J.P., 2001. Nitrogen isotope patterns in the oxygen-deficient waters of the eastern tropical North Pacific Ocean. Deep Sea Res. Part I Oceanogr. Res. Pap. 48, 1905–1921. https://doi.org/10.1016/S0967-0637(00)00110-2.
- Wang, X., Glass, J.B., Reinhard, C.T., Planavsky, N.J., 2019. Species-dependent Cr isotope fractionation across the eastern tropical North Pacific oxygen minimum zone. Geochem. Geophys. Geosyst. 20, 2449–2514 doi: 10.1029/2018GC007883.
- Ward, B.B., Devol, A.H., Rich, J.J., Chang, B.X., Bulow, S.E., Naik, H., Pratihary, A., Jayakumar, A., 2009. Denitrification as the dominant nitrogen loss process in the Arabian Sea. Nature 461, 78–81.
- Yamakawa, A., Yamashita, K., Makishima, A., Nakamura, E., 2009. Chemical separation and mass spectrometry of Cr, Fe, Ni, Zn, and Cu in terrestrial and extraterrestrial materials using thermal ionization mass spectrometry. Anal. Chem. 81, 9787–9794. https://doi.org/10.1021/ac901762a.